Estimating interchannel observation-error correlations for IASI radiance data in the Met Office system

RMetS
Royal Meteorological Society

Estimating interchannel observation-error correlations for IASI radiance data in the Met Office system

L. M. Stewart,[a] S. L. Dance,[b]* N. K. Nichols,[b] J. R. Eyre[c] and J. Cameron[c]
[a]*MetOffice Reading, University of Reading, UK*
[b]*School of Mathematical and Physical Sciences, University of Reading, UK*
[c]*Met Office, FitzRoy Road, Exeter, UK*

*Correspondence to: S. L. Dance, Meteorology Building, University of Reading, RG6 6BB, UK. E-mail: s.l.dance@reading.ac.uk

The optimal utilisation of hyper-spectral satellite observations in numerical weather prediction is often inhibited by incorrectly assuming independent interchannel observation errors. However, in order to represent these observation-error covariance structures, an accurate knowledge of the true variances and correlations is needed. This structure is likely to vary with observation type and assimilation system. The work in this article presents the initial results for the estimation of IASI interchannel observation-error correlations when the data are processed in the Met Office one-dimensional (1D-Var) and four-dimensional (4D-Var) variational assimilation systems. The method used to calculate the observation errors is a post-analysis diagnostic which utilises the background and analysis departures from the two systems.

The results show significant differences in the source and structure of the observation errors when processed in the two different assimilation systems, but also highlight some common features. When the observations are processed in 1D-Var, the diagnosed error variances are approximately half the size of the error variances used in the current operational system and are very close in size to the instrument noise, suggesting that this is the main source of error. The errors contain no consistent correlations, with the exception of a handful of spectrally close channels. When the observations are processed in 4D-Var, we again find that the observation errors are being overestimated operationally, but the overestimation is significantly larger for many channels. In contrast to 1D-Var, the diagnosed error variances are often larger than the instrument noise in 4D-Var. It is postulated that horizontal errors of representation, not seen in 1D-Var, are a significant contributor to the overall error here. Finally, observation errors diagnosed from 4D-Var are found to contain strong, consistent correlation structures for channels sensitive to water vapour and surface properties.

Key Words: satellite observations; 1D-Var; 4D-Var

Received 13 September 2012; Revised 5 June 2013; Accepted 7 June 2013; Published online in Wiley Online Library

1. Introduction

In numerical weather prediction (NWP), the governing equations used to describe the behaviour of the atmosphere are sampled by millions of observations in a 6 h period. Satellite observations are the dominant contributor to the data assimilation algorithms used in global NWP in both quantity and impact on forecast accuracy. Joo *et al.* (2012) shows that a significant contribution to this dominance is given by hyperspectral sounders, such as the Infrared Atmospheric Sounding Interferometer (IASI) and the Atmospheric Infrared Sounder (AIRS), which sample the infrared spectrum using thousands of channels at a close spectral proximity.

The contribution an observation makes to the data assimilation system is governed by the error associated with its measurement and representation; observations with large errors will receive low weighting in the assimilation while those with small errors have a larger impact. Satellite observation errors, including those from hyperspectral sounders, are usually assumed to be uncorrelated in both the horizontal and the vertical. For IASI observations, the assumption of horizontal uncorrelation is supported by intelligent thinning of the data to avoid assimilating observations that are too close spatially.

Ensuring spectrally independent observation errors is more difficult. A measurement in any IASI channel will be sensitive to the temperature and humidity profile over several atmospheric

levels; the distribution being represented by the broad weighting functions of the instrument. Therefore the errors in channels spectrally close to each other are likely to be correlated if some misrepresentation of the observation is common over several levels; for example, the sensitivity to a certain trace gas. Additionally, correlated errors of representation will be present between channels that observe spatial scales or features within the instrument's 12 km field of view which the model does not represent well. Also, any errors in the forward model, such as those of spectroscopy, may be correlated between channels.

The current IASI channel selection procedure attempts to lessen the impact of spectrally correlated errors by avoiding the assimilation of spectrally close channels. But it is generally acknowledged that vertical correlation structure is still present among those channels chosen for assimilation. However, because of a lack of knowledge of the true error correlation structure and the perceived expense of including this structure in the assimilation, the observation errors are treated as uncorrelated between channels. To avoid misweighting the IASI observations in the data assimilation, the error variances are inflated to account for the lack of correlation. The level of inflation for an observation error is determined by the channel in which the measurement was taken. This technique is used at the Met Office, Météo-France and ECMWF to treat IASI observation-error correlations.

Mistreating observation errors as uncorrelated has been shown to be detrimental to the analysis accuracy and information content when using hyperspectral satellite observations (Liu and Rabier, 2003; Rabier *et al.*, 2003; Collard, 2004; Stewart *et al.*, 2008). When used in conjunction with data thinning or channel-constraining algorithms, it inhibits the impact of using greater volumes of satellite data, as shown in Collard (2004) and Dando *et al.* (2007). With the increasing resolution of NWP models, such a restriction on data usage is hardly desirable. This motivated studies into the quantification, and future use in assimilation, of these observation-error correlations.

A number of methods exist for quantifying error correlations in data assimilation; however the application of such methods is not without difficulty. The most commonly used estimation technique is the observational method, often known as the Hollingsworth–Lönnberg method. Hollingsworth and Lönnberg (1986) describe the method which separates background and observation errors using background innovation statistics, under the assumption that the background errors carry spatial correlations while the observation errors do not. With additional inputs, it can be modified to account for correlated errors in the observations. Garand *et al.* (2007) applied the method to AIRS data, showing significant interchannel error correlations. More recently, Bormann and Bauer (2010) and Bormann *et al.* (2010) applied the method to ATOVS (Advanced TIROS Operational Vertical Sounder), AIRS and IASI data used in the ECMWF analysis, again demonstrating considerable correlation structures in certain wavelength bands.

In other techniques, Dee and Da Silva (1999) used a maximum likelihood method to estimate information on error statistics. This work resulted in the derivation of statistical parameters which varied in time. Desroziers and Ivanov (2001) used statistics from analysis innovations to tune background- and observation-error parameters, resulting in a successful description of the observation-error parameters in a 3D-Var framework.

A method that addressed the separation of correlated observation and background errors was proposed in Desroziers *et al.* (2005). This method uses post-analysis diagnostics from linear estimation theory to statistically approximate the covariances of the observation errors. This approach has been used to estimate error variances and interchannel correlations in both the Météo-France (Desroziers *et al.*, 2005) and ECMWF (Bormann *et al.*, 2010) variational assimilation systems. Findings include an overestimation of observation-error variances and strong interchannel correlations at certain wavelengths.

Once observation-error correlations have been quantified, it is useful to be able to identify their sources. As mentioned above, errors in the meteorology, the forward model, and resolution representation can be correlated in the vertical. Current methods make no attempt to calculate the separate contribution from each source of error.

The work described in this article considers the initial application of the Desroziers observation-error diagnostic to estimate the interchannel error correlation structure of IASI observations used in both the Met Office 1D-Var and 4D-Var assimilation system. For each assimilation system, we will compare the diagnosed observation-error variances with those currently used, and establish the level of correlation between the observation errors. Attention will be paid to any variation in structure between different groups of channels. Unlike previous articles on the subject, we will also compare the error variance and correlation structures diagnosed for the two systems, and draw conclusions on the potential origin of the differences. Some results and discussion of this work have been previously presented in Stewart *et al.* (2009) and Stewart (2010).

The article is structured as follows. Firstly in Section 2, we describe the Desroziers technique used to estimate observation-error covariances, and the two assimilation systems which we will be using to process the observations. Section 2 then describes the IASI data used and the experimental set-up. The results are contained in Section 3. Section 3 is separated into the results for processing the IASI observations in 1D-Var, the results for the processing in 4D-Var, and a comparison of the two methods. Finally, a summary and conclusions are given in Section 4.

2. Methodology

Below we describe the methods and data used in this article.

2.1. *Desroziers technique of error approximation*

The technique proposed by Desroziers *et al.* (2005) is based on linear estimation theory, where the optimal analysis describing the true state of the atmosphere, $\mathbf{x}^{\mathrm{a}}$, can be expressed in terms of the background state, $\mathbf{x}^{\mathrm{b}}$, and the background innovation vector, $\mathbf{d}^{\mathrm{o}}_{\mathrm{b}}$,

$$\mathbf{x}^{\mathrm{a}} = \mathbf{x}^{\mathrm{b}} + \mathbf{B}\mathbf{H}^{\mathrm{T}}(\mathbf{H}\mathbf{B}\mathbf{H}^{\mathrm{T}} + \mathbf{R})^{-1}\mathbf{d}^{\mathrm{o}}_{\mathrm{b}}, \tag{1}$$

where $\mathbf{R}$ and $\mathbf{B}$ are the observation- and background-error covariance matrices, respectively, and $\mathbf{H}$ is the Jacobian of the nonlinear observation operator H. The background innovation vector is the difference between the observations, $\mathbf{y}$, and their background counterparts, $H(\mathbf{x}^{\mathrm{b}})$,

$$\mathbf{d}^{\mathrm{o}}_{\mathrm{b}} = \mathbf{y} - H(\mathbf{x}^{\mathrm{b}}). \tag{2}$$

Similarly, the analysis innovation vector, $\mathbf{d}^{\mathrm{o}}_{\mathrm{a}}$, is given by the differences between the observations and their analysis counterparts, $H(\mathbf{x}^{\mathrm{a}})$,

$$\mathbf{d}^{\mathrm{o}}_{\mathrm{a}} = \mathbf{y} - H(\mathbf{x}^{\mathrm{a}}). \tag{3}$$

Desroziers *et al.* (2005) showed that, by taking the statistical expectation, $\mathbb{E}$, of the product of (2) and (3) under the assumption of mutually uncorrelated observation and background errors, an approximation of the observation-error covariance matrix is obtained:

$$\mathbb{E}\left[\mathbf{d}^{\mathrm{o}}_{\mathrm{a}}(\mathbf{d}^{\mathrm{o}}_{\mathrm{b}})^{\mathrm{T}}\right] \approx \mathbf{R}. \tag{4}$$

This relation is satisfied exactly, provided the covariance matrices used in (3) are consistent with the true observation- and background-error covariances. However, given that we know that we are misrepresenting the observation-error covariance structure, Desroziers *et al.* (2005) suggest the use of the estimation technique as an iterative procedure; using the previously

diagnosed **R** matrix at each iteration should result in an **R** matrix closer and closer to reality.

Desroziers *et al.* (2005) used the estimation technique to successfully diagnose background- and observation-error variances for radiosonde wind observations in the French ARPEGE system. For a toy problem, they were also able to tune iteratively observation-error variances and recover observation-error covariances, starting from a mis-specification of both. Bormann and Bauer (2010) and Bormann *et al.* (2010) applied the estimation technique on a larger scale, estimating the error covariance structure for clear-sky sounder radiances used in the ECMWF assimilation system. Results for IASI observations showed noticeable correlation structure in the surface-sensitive and short-wave temperature-sounding channels, and a significant degree of correlation between humidity-sounding channels, provided the correlation scales for the background and observation errors were sufficiently different.

2.2. Assimilation systems

The results presented here will show the interchannel error correlation structure for clear-sky IASI observations processed in the Met Office 1D-Var and 4D-Var systems. The two systems are used together for the processing and assimilation of satellite data in NWP at the Met Office.

The objective of both 1D-Var and 4D-Var retrieval systems is to minimise a cost function that penalises distance from the observations taken at a sequence of times, $\mathbf{y}_i$, and a previous short-range forecast (or background state), $\mathbf{x}^{\mathrm{b}}$,

$$J(\mathbf{x}) = \frac{1}{2}(\mathbf{x}-\mathbf{x}^{\mathrm{b}})^{\mathrm{T}}\mathbf{B}^{-1}(\mathbf{x}-\mathbf{x}^{\mathrm{b}}) + \frac{1}{2}\sum_{i=1}^{n}\{\mathbf{y}_i - H_i(\mathbf{x})\}^{\mathrm{T}}\mathbf{R}_i^{-1}\{\mathbf{y}_i - H_i(\mathbf{x})\}, \tag{5}$$

where n is the total number of observations. The observation operator H_i is comprised of a Radiative Transfer for TIROS Operational Vertical Sounder (RTTOV) radiative transfer model, as described in Matricardi *et al.* (2004) and Saunders *et al.* (2005); it accurately predicts brightness temperatures given first-guess model fields of temperature and humidity, as well as surface air temperature, skin temperature, surface humidity and surface emissivity. The product of the cost function minimisation is an updated estimate of the analysis state of the atmosphere.

The 1D-Var retrieval system, as described in Hilton *et al.* (2009), is used on individual observations prior to their assimilation into the NWP model. It is called by the Observation Processing System (OPS) which is used to pre-screen and quality control the observations. Since the 1D-Var retrieval is applied to single observations, the cost function (5) is minimised with $n = 1$.

One quality control procedure in the OPS identifies observations which are too far from the forecast background and hence may cause problems in the later assimilation. A large value of the cost function (5), or a slow convergence rate, is an indicator of inconsistency between the background forecast and the observations, and hence observations with these attributes are eliminated at this stage. The observations that 'pass' the OPS analysis checks are deemed suitable for assimilation in the Met Office 4D-Var assimilation system (VAR).

The 1D-Var retrieval also provides estimates of the atmospheric variables not represented in 4D-Var but required for radiative transfer calculations. The analysed variables in 4D-Var are a subset of the full state vector variables, and those variables, such as skin temperature, which are not included are unmodifiable. It is therefore crucial to the success of the assimilation that these variables are accurately specified prior to the 4D-Var assimilation. The full state vector, i.e. all variables, is used in the 1D-Var retrieval, and the analysis values of those variables not analysed in 4D-Var are passed there. The first set of statistics in our experiments will be generated using the background, $\mathbf{d}_{\mathrm{b}}^{\mathrm{o}}$, and analysis, $\mathbf{d}_{\mathrm{a}}^{\mathrm{o}}$, innovations from these 1D-Var analyses.

When the 1D-Var retrieval is performed in the OPS, the observation operator (or forward model) is fitted separately to each individual column of observations, so the position of the observations, and hence any resolution conflict, is already determined. Therefore, it can be argued that the horizontal errors of representation, created by a contrast in model and observation resolution, will appear in the background matrix **B**. Hence, the error of representation component of the observation error will be only in the vertical. Therefore, from the 1D-Var diagnostics, we expect observation errors to be predominantly attributed to instrument noise, forward model error and vertical errors of representation.

The 1D-Var retrieval produces a quality controlled subset of brightness temperature measurements suitable for assimilation in the Met Office incremental 4D-Var assimilation system. The 4D-Var retrieval system minimises the cost function (5) over the full sequence of observations, $\mathbf{y}_i$, and assimilates the observations at their measurement times. In 1D-Var, each observation is assimilated at its own horizontal location, while in 4D-Var all the observations are assimilated together at model grid points. A detailed description of the 4D-Var procedure at the Met Office is given in Rawlins *et al.* (2007).

The 4D-Var algorithm generates an optimal analysis increment which is used to update the solution state at the start of the assimilation time window. From this starting state, the nonlinear model is run over the time window to generate the forecast. The forecast model (or analysis) fields are output at model grid points at predetermined times, and can be interpolated to the observation locations. In the 4D-Var assimilation, all observation information is fitted to the resolution provided by the model, and so correlated errors of representation (both horizontal and vertical) are expected to be contained wholly in **R**. The second set of statistics in our experiments will be generated using the analysis innovations from the interpolated analyses, and the background innovations.

The application of the Desroziers diagnostic to both the 1D-Var and 4D-Var analyses estimates the error correlations of the observations used in both systems. However, the diagnosed errors are unlikely to be independent of the system used. While both systems implement a variational assimilation scheme, there are differences in the treatment of the observations. Processes including bias correction, cloud detection, thinning and interaction with background errors, may impact on the diagnostics.

In this work, the bias correction and cloud detection are the same for both sytems; the cloud detection scheme follows that described in English *et al.* (1999) for completely clear scenes. However, the diagnostics may be affected by the difference in the assimilation state vector, the sample of observations and the background errors used. As discussed above, in 1D-Var the full state vector is analysed, while in 4D-Var a subset of this vector is analysed and certain variables are set to the retrieved values from the 1D-Var. In this work, surface skin temperature is the only variable analysed in 1D-Var but not in 4D-Var. Since this work was completed, cloud-top pressure, cloud fraction and land surface emissivity are also pre-analysed in the Met Office 1D-Var system; however, these will not impact on this work. The analysis of fewer variables could potentially lead to exaggerated error correlations in 4D-Var, when small error correlations in 1D-Var (from cloud contamination, for example) are propagated and enlarged in 4D-Var when no modification to affected variables is possible. Also, the 4D-Var diagnostics are calculated from a subset of the data used to calculate the 1D-Var diagnostics, because of additional thinning and processing required to generate the statistics. Therefore, with a smaller sample set, diagnosed correlation features from the 4D-Var diagnostics could be more affected by noise.

In 1D-Var the background-error covariances were generated by interpolating the Met Office 3D-Var background-error covariance

Table 1. Groups of channels by similar spectral properties.

Description	1D-Var channel no.	4D-Var channel no.	IASI channel no. (wavelength, cm^{-1})
Temperature sounding	0–123	0–86	16–457 (648.75–759.00)
Window (surface sensitive)	124–152	87–108	515–2245 (773.50–1206.00)
Water vapour sensitive	148, 150, 153–182	109–138	2019, 2119, 2741–5405 (1149.50, 1174.50, 1330.00–1996.00)

matrix to the pressure levels used in the 1D-Var retrieval. The 3D-Var background-error covariance matrix was generated using a National Meteorological Center (NMC) method to estimate forecast error using differences from a T+24 h and T+48 h operational forecast over a number of days. The background-error covariances in 4D-Var were generated using a NMC method as described in Rawlins *et al.* (2007). In Desroziers *et al.* (2009), it is shown that the ability of the method used in this article to estimate observation errors is dependent on the difference between the assumed observation and background-error correlation length-scales. If the two correlation length-scales are too close, then the algorithm's ability to distinguish between the two sources of error is inhibited. Work examining the impact of different background-error specifications, including using background errors which are tuned to 4D-Var in the 1D-Var system, is ongoing at the Met Office, but is not included in this article.

Because horizontal errors of representation are contained in the observation error in 4D-Var processing but not in 1D-Var processing, we expect that these will be a major contributor to any differences in the diagnosed errors from the two systems. However, errors from the different experimental set-ups of the systems and the different specification of the background-error covariances may also contribute.

2.3. Data

The Desroziers estimation technique described above is applied to data from the IASI instrument on board MetOp-A. IASI is an infrared Fourier transform spectrometer measuring in the spectral interval of 645–2760 cm^{-1} at a resolution of 0.5 cm^{-1}. IASI observations are an important component of the global observing system, and their positive impact on forecasting at the Met Office, ECMWF and Météo-France has been demonstrated in Collard and McNally (2009), Hilton *et al.* (2009), Rabier *et al.* (2009) and Guidard *et al.* (2011).

IASI has the potential to provide observations in 8461 channels, but at the time of the research only observations from a subset of 314 derived in Collard (2007) were used. This subset was chosen under the assumption that error correlations between channels would not be represented. The channels are predominantly in the CO_2 temperature sounding band, with additional channels chosen to provide information on water vapour, trace gases, surface properties, etc. Because of the need to avoid highly correlated channels, the water vapour (WV) band is largely undersampled, despite the need for an accurate representation of humidity structures; the increased use of WV channels was shown to result in a degradation in analysis accuracy in the current framework. Of these 314, 183 channels are used in the 1D-Var assimilation and 139 are used in the 4D-Var assimilation; fewer channels are used in the 4D-Var assimilation since the inclusion of certain channels was found to have a negative impact on analysis accuracy under current conditions. For the 4D-Var statistics, only observations that pass the 1D-Var quality control are used.

Table 1 groups the channels used in 1D-Var and 4D-Var by similar spectral properties. The channels are shown on a typical IASI spectrum in Figure 1 (1D-Var channels) and Figure 2 (4D-Var channels); the different colours represent the different groups of channels.

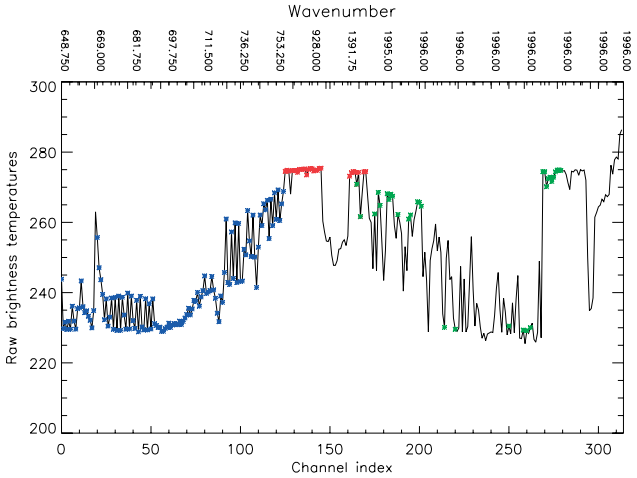

Figure 1. Channels used in 1D-Var on a typical IASI spectrum (K): temperature-sounding channels indexed 0–123 (blue), window channels indexed 124–152 (red), and water vapour channels indexed 148, 150, 153–182 (green).

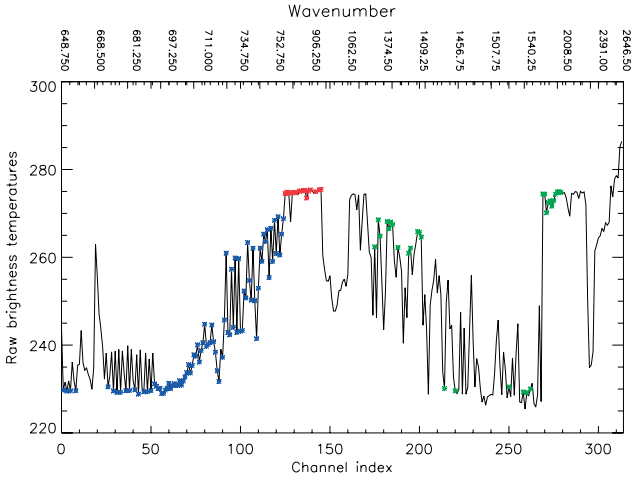

Figure 2. Channels used in 4D-Var on a typical IASI spectrum (K): temperature-sounding channels indexed 0–86 (blue), window channels indexed 87–108 (red), and water vapour channels indexed 109–138 (green).

2.4. Experimental set-up

The Desroziers diagnostic is calculated for two situations: firstly using the analysis output from the 1D-Var retrieval and secondly using the analysis output from the 4D-Var assimilation. The background and analysis increment statistics are generated from the assimilation of only clear-sky, sea surface IASI observations. Observations are from both day- and night-time, with the exception of daytime observations from short-wave channels, which are eliminated. Using only IASI observations in the assimilation makes the diagnosed error structures independent of different observation types. Also, any impact of misweighting the IASI observations will be independent of other observation types in both 1D-Var and 4D-Var.

The 1D-Var results presented here are calculated using 27 854 IASI observations taken on 17 July 2008 from the 6 h cycles at 0000, 0600, 1200 and 1800 UTC. These observations are those

which were suitable for use in the 4D-Var assimilation, prior to the additional observation thinning necessary in this system. Here the 4D-Var results are calculated from a thinned subset of the same IASI observations, but only those taken at 1800 UTC. A total of 2073 observations taken at this time are used in the 4D-Var system. This smaller sample of observations is the result of the extra calculations required after the 4D-Var assimilation had been run. To ensure the same observations are used to generate the $\mathbf{d}_b^o$ innovations (calculated before the assimilation) and the $\mathbf{d}_a^o$ innovations (calculated after the assimilation), we match observations using their latitude and longitide values. This was not necessary for the 1D-Var diagnostics. To support the results generated using this smaller sample size, we performed the same experiments using the same IASI observations from another day. The results from these experiments will not be shown here, but were qualitatively similar to our findings, suggesting that results using this smaller sample size are not overly governed by noise.

In addition to the use of the Desroziers diagnostic, we also use a Hollingworth–Lönnberg method to calculate the error variances from the 4D-Var analyses. A comparison of the two methods for diagnosing observation-error covariances has previously been performed for the ECMWF assimilation system in Bormann *et al.* (2010), and we use it here to verify the robustness of the Desroziers method.

The Hollingsworth and Lönnberg (1986) method typically uses background innovations from a dense observing network to estimate background and observation errors, under the assumption that the background errors carry spatial correlations while the observation errors do not. Observation errors are estimated by calculating innovation covariances for pairs of observations at various separations. By stratifying the covariances as a function of separation distance, the covariance relationship can be extrapolated to zero separation and split into a spatially correlated and spatially uncorrelated component. the latter representing the observation error. Using this method, innovation covariances calculated for the same channel in a pair of observations will provide an estimate of the observation-error variances; innovation covariances calculated for different channels in a pair of observations will tell us about the observation-error covariances.

In this work, the innovation covariances are calculated from pairs of observations whose separation distance is that of the model resolution. A simple Monte Carlo experiment, drawing random pairs of points from boxes similar in size to the model grid, was used to estimate the observation separation representative of the VAR analysis resolution. When the number of pairs was plotted against separation, the mean of the distribution was 84.8 km; this distance was used as the observation separation for the Hollingsworth and Lönnberg calculations. Rather than extrapolating the covariance relationship to zero separation using a correlation function, the innovation covariances at 84.8 km were subtracted from those at close to zero separation. The difference is taken to represent the observation-error component of the covariance. A similar method used in Bormann and Bauer (2010) was shown to give more robust results than the use of a correlation function.

3. Results

In this section we present the observation-error structures derived when IASI observations are assimilated in the Met Office 1D-Var and 4D-Var systems. The observation errors are derived using the Desroziers technique described in Section 2.1. Comparisons are made with the operational observation-error variances, and the observation-error correlation matrices are calculated. Diagnosed interchannel correlation structures will be compared for the two retrieval systems, and conclusions will be drawn as to the origin of the observation-error correlations.

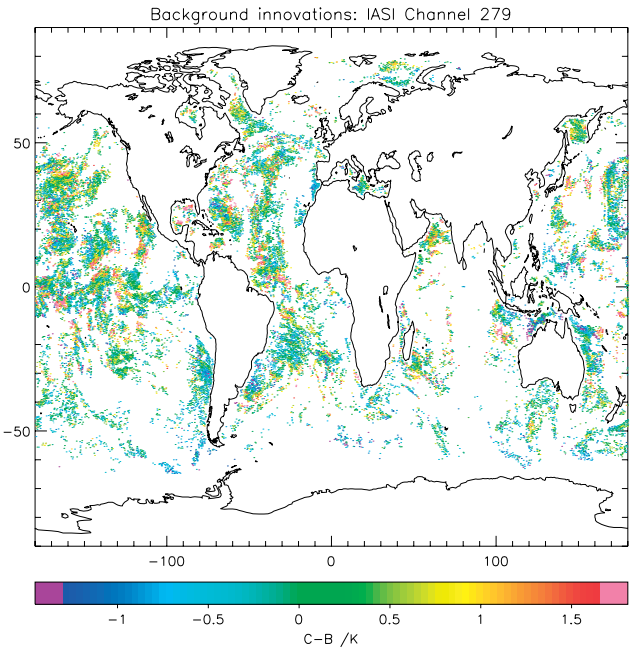

Figure 3. Global location and background innovation value $O-B$ (K) for observations in IASI channel 5403.

3.1. 1D-Var assimilation

First we consider the application of the Desroziers diagnostic to the 1D-Var analyses. Figure 3 shows the global location of all the observations used in the 1D-Var retrieval, and the size of their background innovations for IASI channel 5403, which is highly sensitive to WV.

The observation-error variances calculated using the Desroziers diagnostic, the operational error variances used in 1D-Var at the Met Office, and an approximation of the IASI instrument noise are shown in Figure 4. The operational error variances are comprised of the instrument noise plus a forward model error of 0.2 K^2. Results are shown for the 183 channels used in the 1D-Var retrieval.

The structure of the operational and diagnostic error variances in Figure 4 is very similar, but the diagnosed error variance is noticeably lower than the operational error variance for all channels. The largest difference is in the indexed channels 148–180 which are highly sensitive to WV. Also the diagnosed error variances are very close in size to the instrument noise. This suggests that the forward model component of the error variances is being overestimated in 1D-Var, especially in channels sensitive to WV, and that a large part of the true observation error is from the instrument noise.

Once the observation error covariances are calculated, the error correlation matrix, $\mathbf{C}$, can be determined easily from the error covariance matrix using the identity $\mathbf{R} = \mathbf{D}^{1/2}\mathbf{C}\mathbf{D}^{1/2}$ where $\mathbf{D}$ is the diagonal matrix of error variances. The diagnosed error correlation matrix for the 183 channels used in the 1D-Var retrieval is shown in Figure 5. Noticeably, the correlation structure is not uniformly symmetric, which is a necessity for an error correlation matrix. However, this is expected since we are violating one of the diagnostic assumptions by using an error covariance matrix which is not entirely representative of the true error structure, i.e. $\mathbf{R}$ operational $\neq \mathbf{R}$ truth. Potentially an iterative procedure for updating the error variances, as proposed in Desroziers *et al.* (2005), would make the error covariance matrix $\mathbf{R}$ closer to symmetric as we moved closer to using the true error correlation matrix; however this will be influenced by the specification of the background-error covariance matrix.

Looking at the error correlations in Figure 5, we observe that in the temperature-sounding channels, indexed below 120, there is little identifiable correlation structure with the exception of two channels which are strongly correlated with their neighbours (IASI

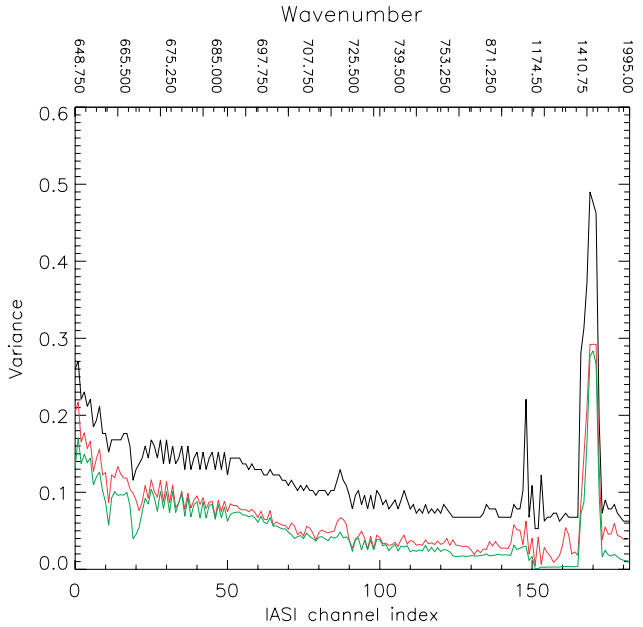

Figure 4. Operational error variances (K^2) (black line), diagnosed error variances (red line) and instrument noise (green line).

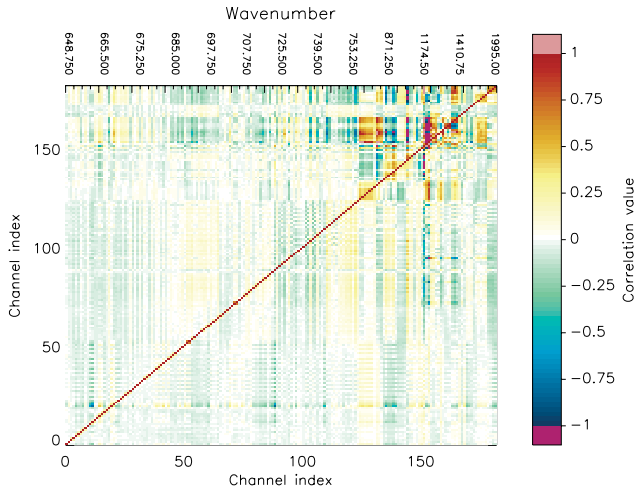

Figure 5. Diagnosed observation-error correlation matrix for the 183 channels used in 1D-Var. The wavenumber of the channels is given on the top axis and the colour bar indicates correlation value.

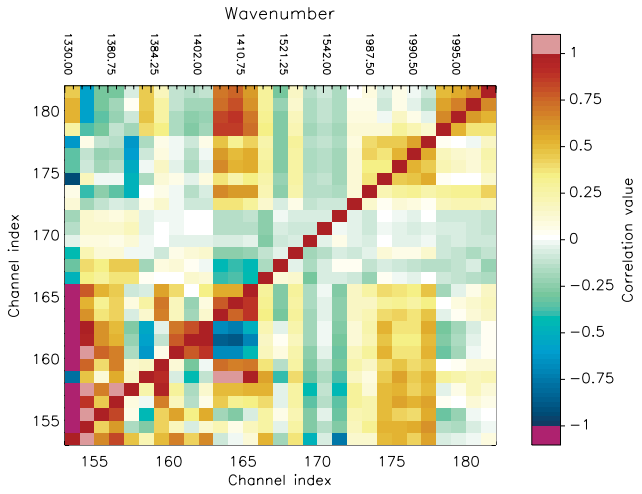

Figure 6. Diagnosed observation-error correlation matrix for WV-sensitive channels used in 1D-Var (Table 1 gives corresponding IASI channel numbers). The wavenumber of the channels is given on the top axis and the colour bar indicates correlation value. Correlations displaying a value of greater than 1 are a result of rounding error, and represent a value very close to 1.

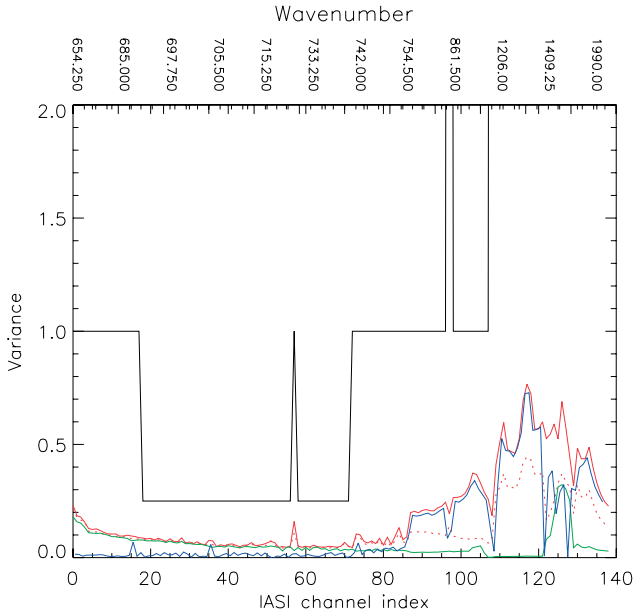

Figure 7. Operational error variances (K^2) (black line), diagnosed error variances (red line) and the first off-diagonal covariance (blue line), Hollingsworth–Lönnberg diagnosed error variances (red dashed line) and instrument noise (green line).

channels 180 and 243, wavelength 689.75 cm^{-1} and 705.50 cm^{-1}, respectively). These two channels were chosen for monitoring purposes and are spectrally closer to their neighbours than the other temperature-sounding channels (0.25 cm^{-1} compared with 0.5 cm^{-1}); hence they are strongly correlated because of the apodisation applied to IASI data. In the WV-sensitive channels there is some significant correlation structure. However, there does not appear to be any consistent correlation between channels with similar properties. This can be seen more clearly in Figure 6 which provides a close-up of the error correlation structure for the WV-sensitive channels. There are a few small blocks of correlation structure corresponding to channels very close together on the spectrum (Figure 1), but the majority of correlation structure appears incoherent.

We can conclude that, when the IASI observations are analysed using 1D-Var statistics, the errors lack any consistent correlation, with the exception of a small number of neighbouring channels sensitive to WV. Figure 4 showed the closeness of the derived error variances to the instrument noise, suggesting that this plus some forward model error was the main contributor to the overall observation error in 1D-Var. We can therefore surmise that these error sources are largely independent of IASI channel choice.

3.2. *4D-Var assimilation*

We now calculate the observation-error covariances using the analysis innovations derived from the 4D-Var assimilation of IASI data.

Figure 7 shows the observation-error variances used in 4D-Var (black line), the instrument noise (green line), the error variances (red line) and first off-diagonal (blue line) from the symmetrised matrix diagnosed using the Desroziers method, $\mathbf{R}_{\mathrm{sym}} = \frac{1}{2}(\mathbf{R} + \mathbf{R}^{\mathrm{T}})$, and the error variances diagnosed using the modified Hollingsworth–Lönnberg method as described in Section 2.4 (red dashed line). The values out of range are for channels where the operation-error variance is 4.0. For all channels the diagnosed error variances from the Desroziers method are significantly smaller than those being used operationally, implying that the error variances are heavily overestimated. However, the size of the first off-diagonal covariance value indicates why this overestimation is necessary. For the majority of the window and WV channels used in the 4D-Var assimilation, the first off-diagonal covariance value is very

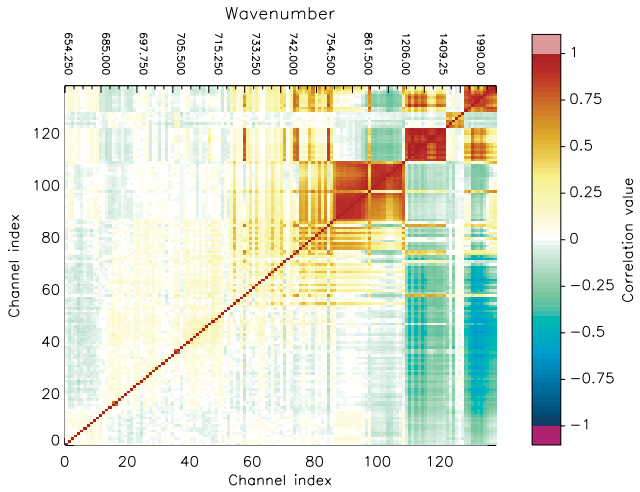

Figure 8. Diagnosed observation-error correlation matrix for the 139 channels used in 4D-Var. The wavenumber of the channels is given on the top axis and the colour bar indicates the correlation value.

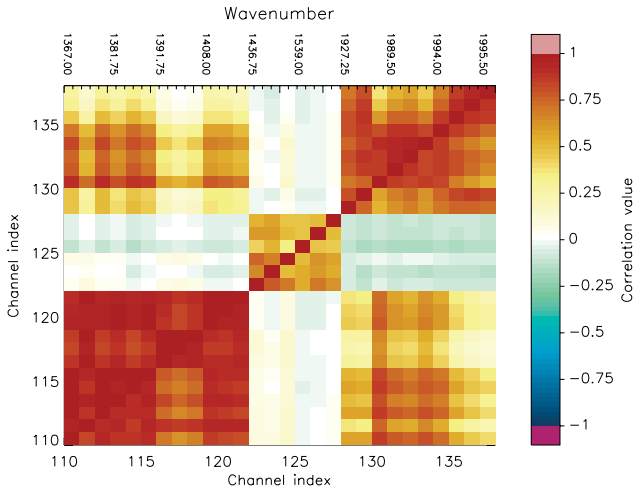

Figure 9. Diagnosed observation-error correlation matrix for WV-sensitive channels used in 4D-Var (Table 1 gives corresponding IASI channel numbers). The wavenumber of the channels is given on the top axis and the colour bar indicates the correlation value.

close in size to the diagonal variance value; therefore ignoring this value and other off-diagonal elements will result in the incorrect overweighting of the observations in the analysis. We conclude that it is necessary to inflate the error variances if the large off-diagonal covariances are ignored.

Interestingly, the diagnosed error variances are significantly larger than the instrument noise for surface and WV-sensitive channels; for some WV-sensitive channels, the instrument noise is less than a fifth of the total error variance. We can conclude that instrument noise is not the main source of error in these channels when IASI observations are assimilated in 4D-Var. For much of the temperature-sounding channels, the instrument noise appears to make up the main contribution to the diagnosed error, as with the 1D-Var results.

Comparing the error variances diagnosed with the Desroziers technique with those derived using the Hollingsworth–Lönnberg method, we observe that the latter method produces very similar error variances for the temperature-sounding channels, and slightly smaller error variances for the window and WV channels. Although the Hollingsworth–Lönnberg variances are smaller in these latter channels, the magnitudes are comparable with those derived using the Desroziers technique and are much smaller than those currently being used. The results vary slightly from those found in Bormann *et al.* (2010) where the Hollingsworth–Lönnberg method produced slightly larger error variances than the Desroziers technique. This is potentially due to the different observation separations used to calculate the innovation covariances. However, the similarities in the magnitude of the diagnosed errors compared to those used operationally gives us confidence in the robustness of the Desroziers results.

Figure 8 shows the diagnosed observation-error correlations for the 139 channels used in the 4D-Var retrieval. There are four significant block structures of correlation centred around the diagonal: the first is for the window channels, and the latter three for channels sensitive to WV in different parts of the spectrum. These four groups of channels are easily identifiable on the typical IASI spectrum shown in Figure 2. The block error structure suggests strongly correlated errors within the window and WV channels in similar parts of the spectrum.

Figure 9 shows a closer look at the three blocks of WV-sensitive channels. Many of the most strongly correlated channels have error correlations larger than 0.75. We also observe that not all WV channels are highly correlated; it is channels in similar parts of the spectrum (i.e. long-wave and short-wave) and with similar sensitivity to WV that are the most strongly correlated. Finally, bands of strong correlation are also visible surrounding the first, and largest, block structure in Figure 8. These bands are for

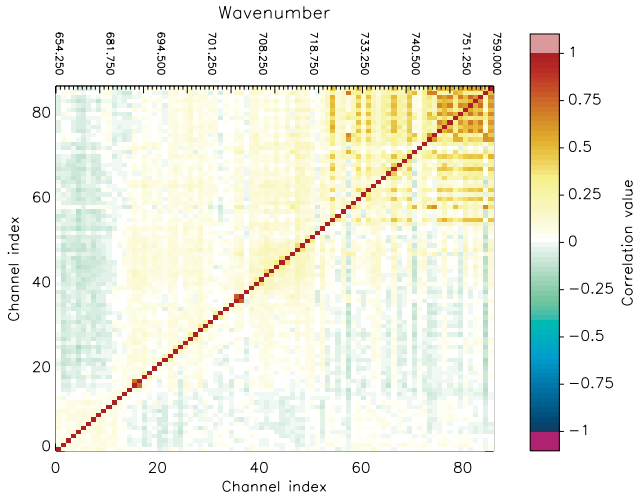

Figure 10. Diagnosed observation-error correlation matrix for the temperature-sounding channels used in 4D-Var (Table 1 gives corresponding IASI channel numbers). The wavenumber of the channels is given on the top axis and the colour bar indicates the correlation value.

channels in the temperature-sounding part of the spectrum with a higher than average sensitivity to WV.

Although correlations are largest in those channels highly sensitive to WV or surface properties, a weaker level of correlation is also present in the channels used in temperature sounding. Figure 10 shows two fainter blocks of correlation centred on the diagonal for the upper temperature-sounding channels (indexed channels 0–50), in addition to bands of correlations for the WV-sensitive lower temperature sounding channels (indexed channels 51–86). Many channels within these two blocks are spectrally close to each other, and therefore we would expect some level of error correlation structure. The differences in measurements between these channels can be used to capture fine-scale information on humidity and temperature profiles; it is therefore desirable to include even a weak level of correlation structure in an attempt to lower the operational error variances and hence retain more information.

The results from 4D-Var are similar to those found in Bormann *et al.* (2010). For channels strongly sensitive to the surface or WV, observation errors larger than the instrument noise, but considerably smaller than the operational error variances, were diagnosed using the Desroziers method amongst others. Strong interchannel error correlations were also present between these channels, which were not seen to the same extent in the temperature-sounding band.

3.3. Comparison of 1D-Var and 4D-Var results

As described in Section 2.2, IASI observations in the Met Office system are initially processed in a 1D-Var retrieval before their use in the forecast model using a 4D-Var assimilation method. We are interested in how the observation-error covariances vary with these two procedures.

When IASI observations are processed in 1D-Var, we expect the observation errors to be largely made up of forward model error and instrument noise, with some vertical error of representation. The diagnosed observation-error variances were shown to be very close to the instrument noise for most of the channels used, implying that most of the error comes from this source, with a small contribution from the forward model error and vertical errors of representation (Figure 4).

In a 4D-Var assimilation, errors of representation in the horizontal also contribute to the observation-error covariance matrix. When the IASI observations are processed in the 4D-Var retrieval, the diagnosed observation-error variances were much larger than the instrument noise in channels sensitive to surface properties and WV (Figure 7). This suggests that instrument noise is no longer the main contributing factor to the errors in these channels, as in 1D-Var. The remaining error can be attributed to horizontal errors of representation, which contribute in a 4D-Var analysis but not in a 1D-Var retrieval, minus those errors caused by inconsistency between the 1D-Var and 4D-Var experimentation. These include (i) different observation sample sizes, (ii) different skin temperature specification, and (iii) different background errors.

Considering the potential error sources, firstly, the smaller observation sample size used in calculating the 4D-Var diagnostics was supported by additional experiments, so we expect this not to be a significant contributor to any error differences. Secondly, in 1D-Var, skin temperature is included in the state vector for retrieval, while in 4D-Var it is not and a fixed value is used. One of the functions of the 1D-Var retrieval is to estimate accurately variables not modifiable in 4D-Var; this avoids a poorly specified skin temperature value being used in 4D-Var and causing the misinterpretation of atmospheric information for surface-sensitive channels. Hence, the retrieval of skin temperature in 1D-Var has the potential to affect the error diagnostics for surface-sensitive channels in 4D-Var.

Finally, provided an accurate value of skin temperature is given, the different background errors used in 1D-Var and 4D-Var will likely contribute to any error differences not attributable to horizontal errors of representation. The 4D-Var error diagnostics may benefit from the different correlation structure in the assumed observation and background errors for this assimilation method; the former are assumed to be spatially uncorrelated and the latter are assumed to include spatial correlations. Indeed a difference in correlation length-scale between the two types of errors was shown to improve error variance diagnosis in Desroziers *et al.* (2009). However, in the 1D-Var retrieval, spatial error correlations are not present by design, so there is no difference in observation- and background-error correlation length-scales to be utilised. We do not attempt here to quantify the impact of skin temperature and background-error specification, but we recognise their potential contribution to the differences in the observation errors diagnosed in the two systems.

Comparing the derived error variances with those used operationally, we observe that the overestimation of the operational error variances in 4D-Var was much larger than that seen in the 1D-Var results. In 1D-Var the overestimation was approximately double the diagnosed error variances (Figure 4), while in 4D-Var the overestimation is up to 8 times the diagnosed error variance for the WV-sensitive channels (Figure 7).

The observation errors calculated from the 1D-Var statistics were shown to contain little consistent strong correlation (Figure 5), with the exception of a handful of spectrally close WV-sensitive channels. However, when statistics from 4D-Var were used in error diagnostics, strong correlations were diagnosed for channels sensitive to WV and surface properties (Figure 8). Many of the strongly correlated channels had correlations larger than 0.75; the error correlations in 1D-Var were rarely at this level.

However, not all the WV-sensitive channels used in the 4D-Var assimilation had highly correlated errors; it was channels with similar spectral properties and sensitivity to WV that were the most strongly correlated. This again is different to the 1D-Var results, where there was little consistency of correlation within the long-wave and short-wave WV channels. For the temperature-sounding channels, as with the WV-sensitive channels, the consistency and level of error correlation structure is far greater in the 4D-Var results than in those derived from 1D-Var statistics.

4. Summary and conclusions

In order to model successfully observation-error correlations, an accurate knowledge of the true correlation structure is needed. This structure varies with observation type and, as shown here, assimilation system. In this article we present the initial results from using a post-analysis diagnostic derived from variational data assimilation theory to calculate IASI observation-error correlations when the data are used in the 1D-Var and 4D-Var assimilation systems at the Met Office.

The need for an accurate specification of error correlation structure when assimilating high-resolution satellite data has become increasingly important in recent years. A number of methods exist for quantifying error correlations, and have been applied for different data types and operational frameworks. In this article we use the Desroziers technique of error approximation, and compare the diagnosed error variances and correlations with those used in the current operational system.

When IASI observations are analysed in the Met Office 1D-Var retrieval system, the diagnosed error variances are approximately half the size of the current operational error variances and are very close in size to the instrument noise. The errors also contain little consistent strong correlation, with the exception of a handful of neighbouring WV-sensitive channels. We conclude that current operational errors are being overestimated, and that uncorrelated instrument noise is the main contributor to the observation error.

When the IASI observations are processed in the Met Office 4D-Var retrieval system, we again found that the observation errors were being overestimated operationally. However, using this assimilation system resulted in an overestimation of up to eight times in channels highly sensitive to WV. The diagnosed errors were noticeably larger than the instrument noise for surface and WV-sensitive channels, suggesting that other error sources had a significant contribution. Because horizontal errors of representation are expected in 4D-Var processing but not in 1D-Var processing, these are a likely contributor to the additional error; errors from pre-processing and the specification of the background-error covariances may also contribute.

Also, the diagnosed errors from 4D-Var were found to contain significant correlation structure. The findings can be broken down into three main features: (i) a strong consistent block correlation structure in the WV- and surface-sensitive channels, (ii) bands of correlation in the temperature-sounding channels sensitive to WV, and (iii) a weaker but still significant level of block correlation structure in the upper temperature-sounding channels. The results were similar to those found by Bormann *et al.* (2010), who identified large and spatially correlated errors in surface and WV-sensitive channels. We can conclude that, in the 4D-Var assimilation system, observation errors are again being overestimated, and strong correlations within the WV- and surface-sensitive channels are being ignored.

Finally, there were several differences in the diagnosed errors from the 1D-Var and 4D-Var statistics. These can be summarised as:

- the source of the observation error was predominantly instrument noise in 1D-Var, while in 4D-Var additional sources of error, including horizontal errors of representation, made a significant contribution;
- the overestimation of the error variances was much larger in 4D-Var for many of the channels used;
- the error correlation structure is much stronger and more consistent between channels with similar spectral properties in 4D-Var.

We can conclude that the assimilation method used to process the observations has a significant impact on the size and structure of the observation-error correlations diagnosed.

We have been able to draw some interesting conclusions from the findings above, but it is important to note that the Desroziers diagnostic is not unflawed. The lack of symmetry in the diagnosed error covariance and correlation matrices is a visual indicator that some of the assumptions used in the derivation of the diagnostic have been violated. We are knowingly using an incorrect observation-error covariance matrix in both assimilation systems, and we suspect that the operational background-error covariance matrices used are also different to the truth. This is expected to lead to asymmetry.

Other potential issues are channel selection choice and observation sampling. The work above was undertaken when there was a fixed IASI channel selection for 1D-Var and 4D-Var; currently the channel selection choice is adaptive and dependent on additional quality control related to cloudy fields of view. This does not affect the use of the diagnostic nor the substance of the results presented here; it requires only a modification of the application. Also, the statistics used in the calculation of the covariance matrices were taken from a global sample, and hence local effects could be masked. But it is not proposed that we use these exact diagnosed error structures in the Met Office assimilation system; instead that they provide the motivation and framework for future investigations.

When the work in this article was undertaken, the operational treatment of interchannel IASI observation errors at the Met Office was to assume independent interchannel errors in both 1D-Var and 4D-Var. The findings from this work challenge the validity of this assumption. Motivated by these results, Weston (2011) describes the work at the Met Office currently under way on using error covariances diagnosed using the Desroziers method in the 4D-Var assimilation system. One important question being addressed is whether it is possible to include all diagnosed correlation structure, or whether an approximation to the derived structure is necessary for computational purposes. It is expected that a better understanding, and hence representation, of the observation-error structures in 1D-Var and 4D-Var will improve the use of IASI data in the Met Office processing systems.

References

Bormann N, Bauer P. 2010. Estimates of spatial and interchannel observation-error characteristics for current sounder radiances for numerical weather prediction. I: Methods and application to ATOVS data. *Q. J. R. Meteorol. Soc.* **136**: 1036–1050.

Bormann N, Collard AD, Bauer P. 2010. Estimates of spatial and interchannel observation-error characteristics for current sounder radiances for numerical weather prediction. II: Application to AIRS and IASI data. *Q. J. R. Meteorol. Soc.* **136**: 1051–1063.

Bouttier F, Kelly G. 2001. Observation-system experiments in the ECMWF 4D-Var data assimilation system. *Q. J. R. Meteorol. Soc.* **127**: 1469–1488.

Collard AD. 2004. 'On the choice of observation errors for the assimilation of AIRS brightness temperatures: A theoretical study'. Technical Memorandum AC/90. ECMWF: Reading, UK.

Collard AD. 2007. Selection of IASI channels for use in Numerical Weather Prediction. *Q. J. R. Meteorol. Soc.* **133**: 1977–1991.

Collard AD, McNally AP. 2009. The assimilation of Infrared Atmospheric Sounding Interferometer radiances at ECMWF. *Q. J. R. Meteorol. Soc.* **135**: 1044–1058.

Dando ML, Thorpe AJ, Eyre JR. 2007. The optimal density of atmospheric sounder observations in the Met Office NWP sytem. *Q. J. R. Meteorol. Soc.* **133**: 1933–1943.

Dee DP, Da Silva AM. 1999. Maximum-likelihood estimation of forecast and observation error covariance parameters. Part 1: Methodology. *Mon. Weather Rev.* **127**: 1822–1834.

Desroziers G, Berre L, Chapnik B. 2009. 'Objective validation of data assimilation systems: diagnosing sub-optimality'. In *Proceedings of seminar on diagnosis of forecasting and data assimilation systems*, ECMWF, Reading, UK, 7–10 September 2009. Available from http://www.ecmwf.int/publications/library/ecpublications/pdf/ seminar/2009/Desroziers.pdf.

Desroziers G, Berre L, Chapnik B, Poli P. 2005. Diagnosis of observation, background and analysis-error statistics in observation space. *Q. J. R. Meteorol. Soc.* **131**: 3385–3396.

Desroziers G, Ivanov S. 2001. Diagnosis and adaptive tuning of observation error parameters in variational assimilation. *Q. J. R. Meteorol. Soc.* **127**: 1433–1452.

English SJ, Eyre JR, Smith JA. 1999. A cloud-detection scheme for use with satellite sounding radiances in the context of data assimilation for numerical weather prediction. *Q. J. R. Meteorol. Soc.* **125**: 2359–2378.

Garand L, Heilliette S, Buehner M. 2007. Interchannel error correlation associated with AIRS radiance observations: Inference and impact in data assimilation. *J. Appl. Meteorol.* **46**: 714–725.

Guidard V, Fourrié N, Brousseau P, Rabier F. 2011. Impact of IASI assimilation at global and convective scales and challenges for the assimilation of cloudy scenes. *Q. J. R. Meteorol. Soc.* **137**: 1975–1987.

Hilton F, Atkinson NC, English SJ, Eyre JR. 2009. Assimilation of IASI at the Met Office and assessment of its impact through observing system experiments. *Q. J. R. Meteorol. Soc.* **135**: 495–505.

Hollingsworth A, Lönnberg P. 1986. The statistical structure of short-range forecast errors as determined from radiosonde data. Part 1: The wind field. *Tellus* **38A**: 111–136.

Joo S, Eyre JR, Marriott R. 2012. 'The impact of Metop and other satellite data within the Met Office global NWP system using an adjoint-based sensitivity method'. Forecasting Research Technical Report562. Met Office: Exeter, UK.

Liu Z-Q, Rabier F. 2003. The potential of high-density observations for numerical weather prediction: A study with simulated observations. *Q. J. R. Meteorol. Soc.* **129**: 3013–3035.

Matricardi M, Chevallier F, Kelly G, Thepaut J-N. 2004. An improved general fast radiative transfer model for the assimilation of radiance observations. *Q. J. R. Meteorol. Soc.* **130**: 153–173.

Rabier F, Fourrié N, Chafai D, Prunet P. 2002. Channel selection methods for Infrared Atmospheric Sounding Interferometer radiances. *Q. J. R. Meteorol. Soc.* **128**: 1011–1027.

Rabier F, Bouchard A, Faccani C, Fourrié N, Gerard E, Guidard V, Guillaume F, Karbou F, Moll P, Payan C, Poli P, Puech D. 2009. 'Global impact studies at Météo-France'. Available from http://www.crnm.meteo.fr/gmap/sat/Glocal-Studies-MF.pdf.

Rawlins F, Ballard SP, Bovis KJ, Clayton AM, Li D, Inverarity GW, Lorenc AC, Payne TJ. 2007. The Met Office global four-dimensional variational data assimilation scheme. *Q. J. R. Meteorol. Soc.* **133**: 347–362.

Saunders R, English SJ, Francis P, Rayer P, Brunel P, Kelly G, Bauer P, Salmond D, Dent D. 2005. 'RTTOV-8 the latest update to the RTTOV model'. In *Proceedings of International TOVS Study Conference XIV*, Beijing, China, 25–31 May 2005. Available from http://cimss.ssec.wisc.edu/itwg/itsc/itsc14/proceedings.

Stewart LM. 2010. 'Correlated observation errors in data assimilation'. PhD thesis, University of Reading, UK. Available from http://www.reading.ac.uk/maths-and-stats/research/maths-phdtheses.aspx.

Stewart LM, Dance SL, English SJ, Eyre JR, Nichols NK. 2009. 'Observation error correlations in IASI radiance data'. Mathematical Report Series 1/2009. University of Reading: UK. Available from http://www.rdg.ac.uk.maths/research/maths-report-series.aspx.

Stewart LM, Dance SL, Nichols NK. 2008. Correlated observation errors in data assimilation. *Int. J. Numer. Meth. Fluids* **56**: 1521–1527.

Weston P. 2011. 'Progress towards the implementation of correlated observation errors in 4D-Var'. Forecasting Research Technical Report 560. Met Office: Exeter, UK.